Lithos 114 (2010) 413–422

Contents lists available at ScienceDirect

Lithos

journal homepage: www.elsevier.com/locate/lithos

Anorthitic plagioclase and pargasitic amphibole in mantle peridotites from the Yungbwa ophiolite (southwestern Tibetan Plateau) formed by hydrous melt metasomatism

Chuan-Zhou Liu [a,*], Fu-Yuan Wu [a], Simon A. Wilde [b], Liang-Jun Yu [a], Ji-Liang Li [a]

[a] State Key laboratory of Lithospheric Evolution, Institute of Geology and Geophysics, Chinese Academy of Sciences, Beijing, 100029, China
[b] Department of Applied Geology, Western Australian School of Mines, Curtin University of Technology, Bentley, Western Australia 6102, Australia

ARTICLE INFO

Article history:
Received 19 March 2009
Accepted 2 October 2009
Available online 20 October 2009

Keywords:
Anorthitic plagioclase
Pargasite
Melt metasomatism
Ophiolite
Indus–Yarlung Zangbo Suture
Tibetan Plateau

ABSTRACT

Plagioclase crystals with an anorthite content up to An_{99} have been discovered in mantle peridotites from the Yungbwa ophiolite, which crops out along the Indus–Yarlung Zangbo Suture, southwestern Tibetan Plateau. Amphiboles of pargasitic composition also occur in these plagioclase peridotites. Microtextures support the view that both plagioclase and amphibole were formed metasomatically by hydrous melts entering the Yungbwa peridotites, during which pyroxene was dissolved and olivine was precipitated. The extreme Ca-rich nature of the plagioclase indicates that the metasomatic melts had high Ca/Na ratios, whereas low Ti contents in accompanying spinel and amphibole indicate severe depletion of Ti in the hydrous melts. This suggests that the metasomatic melts were derived from a refractory mantle source. Clinopyroxene trace element data indicate that the metasomatic melts were also enriched in light rare earth elements relative to both middle and heavy rare earth elements. Therefore, the melts show geochemical characteristics similar to arc magmas. This implies that the mantle peridotites in the Yungbwa ophiolite experienced a two-stage evolution; they were formed at a mid-ocean ridge and subsequently entered a subduction zone setting. Their history thus records the opening and closing of the Neo-Tethys Ocean.

1. Introduction

Plagioclase has been widely reported in mantle peridotites from a range of tectonic settings, including ophiolitic peridotites (Dijkstra et al., 2003; Müntener et al., 2004; Borghini et al., 2007; Piccardo et al., 2007), orogenic peridotites (Takazawa et al., 2000) and abyssal peridotites (Hamlyn and Bonatti, 1980; Dick, 1989; Cannat and Seyler, 1995; Constantin, 1999; Pearce et al., 2000; Seyler et al., 2001; Hellebrand et al., 2002a; Tartarotti et al., 2002). Plagioclase-bearing peridotites comprise an important component of abyssal peridotites on the seafloor. For example, it has been estimated that plagioclase peridotites represent about 20% by volume of all peridotites dredged from the ocean floor (Dick, 1989). To date, there is no consensus on the mechanism of plagioclase formation in mantle peridotites and two contrasting processes have been proposed: (1) it represents the breakdown products of spinels at low pressures; (2) it formed through melt impregnation of spinel peridotites. In the first process, plagioclase peridotites are simply residues of melt depletion. Plagioclase is produced in a closed system through sub-solidus breakdown of spinel according to the reaction: clinopyroxene + orthopyroxene + spinel → plagioclase + olivine (Green and Hibberson, 1970; Rampone et al., 1993). The second process, however, takes place in an open system with the involvement of exotic melts. Plagioclase peridotites formed in this way tend to have higher contents of both Na and Ti compared to the residual spinel peridotites. For example, it has been demonstrated that the Ti content of plagioclase-bearing abyssal peridotites from the Romanche Fracture Zone (Atlantic Ocean) reflects binary mixing between residual spinel peridotite and basaltic melt (Dick, 1989).

Anorthitic plagioclase, by definition, has an anorthite content [An = molar Ca/(Ca + Na)] greater than 90%. It has been discovered in volcanic and plutonic mafic rocks (Falloon and Green, 1986; Sinton et al., 1993; Nielsen et al., 1995; Lundstrom and Tepley, 2006), but rarely in mantle peridotites (Hamlyn and Bonatti, 1980; Arai, 1991; Cannat and Seyler, 1995; Rampone et al., 1997; Franz et al., 2002). As indicated above, just how anorthitic plagioclase can form in mantle peridotites is subject to debate. Plagioclase with a composition of almost pure anorthite (An~98) has been previously reported in mantle wedge xenoliths from Papua New Guinea and interpreted to be of metasomatic origin (Franz et al., 2002).

Plagioclase with a composition of An_{99}, in association with pargasitic amphibole, has recently been discovered in mantle peridotite from the Yungbwa ophiolite, southwestern Tibetan Plateau. In this study, we present mineralogical and chemical data to support

* Corresponding author. Tel.: +86 10 82998547; fax: +86 10 62010846.
E-mail address: chzliu@mail.iggcas.ac.cn (C.-Z. Liu).

0024-4937/$ – see front matter © 2009 Elsevier B.V. All rights reserved.
doi:10.1016/j.lithos.2009.10.008

the metasomatic origin of this unusual association. We then use the chemical characteristics of the inferred metasomatic melts to discuss the evolution of the Yungbwa ophiolite.

2. Geological setting

The Tibetan Plateau was formed by the northward accretion of several terranes, separated by well-defined suture zones (Yin and Harrison, 2000). The Indus–Yarlung Zangbo Suture is the southernmost of these, separating the Lhasa block of the Eurasian plate to the north from the Indian plate to the south. Nearly continuous E–W trending ophiolitic massifs crop out along the Indus–Yarlung Zangbo Suture, including the Luobusha ophiolite and Xigaze ophiolite in the eastern and central segments, respectively. In earlier studies, they were considered analogues of oceanic lithosphere, of mid-ocean ridge affinity (Nicolas et al., 1981; Girardeau et al., 1985a,b; Girardeau and Mercier, 1988; Pearce and Deng, 1988). However, more recently a consensus has been reached that most, if not all, ophiolites along the Indus–Yarlung Zangbo Suture are related to supra-subduction zone settings (Zhou et al., 1996; Hébert et al., 2003; Malpas et al., 2003; Xia et al., 2003; Dubois-Côté et al., 2005; Zhou et al., 2005).

The Yungbwa ophiolite is the largest ophiolite found along the western segment of the Indus–Yarlung Zangbo Suture (Fig. 1). This ophiolite is characterised by the occurrence of a large peridotite body (ca. 700 km^2) with some associated crustal rocks, which tectonically overlies an Upper Cretaceous mélange that includes a wide variety of exotic sedimentary and volcanic blocks (Miller et al., 2003; Xu et al., 2006). The mantle sequence consists of harzburgite, lherzolite and minor dunites. Locally, magmatic veins with compositions ranging from pyroxenite to gabbronorite cross-cut the mantle peridotites.

3. Petrography

The three samples selected in the present study were collected from the largest mantle peridotite body of the Yungbwa ophiolite (30°35.643′N, 81°16.952′E), and all are remarkably fresh with little serpentinisation. They are composed of clinopyroxene-bearing harzburgites, in which the modal content of olivine varies from 65 to 70%, orthopyroxene from 25 to 28%, clinopyroxene from 3 to 5% and spinel less than 0.5%. Both plagioclase and amphibole were discovered in all three samples, but with modal contents less than 0.5%.

All samples display porphyroclastic textures resulting from plastic deformation. The olivine porphyroclasts show elongate shapes with

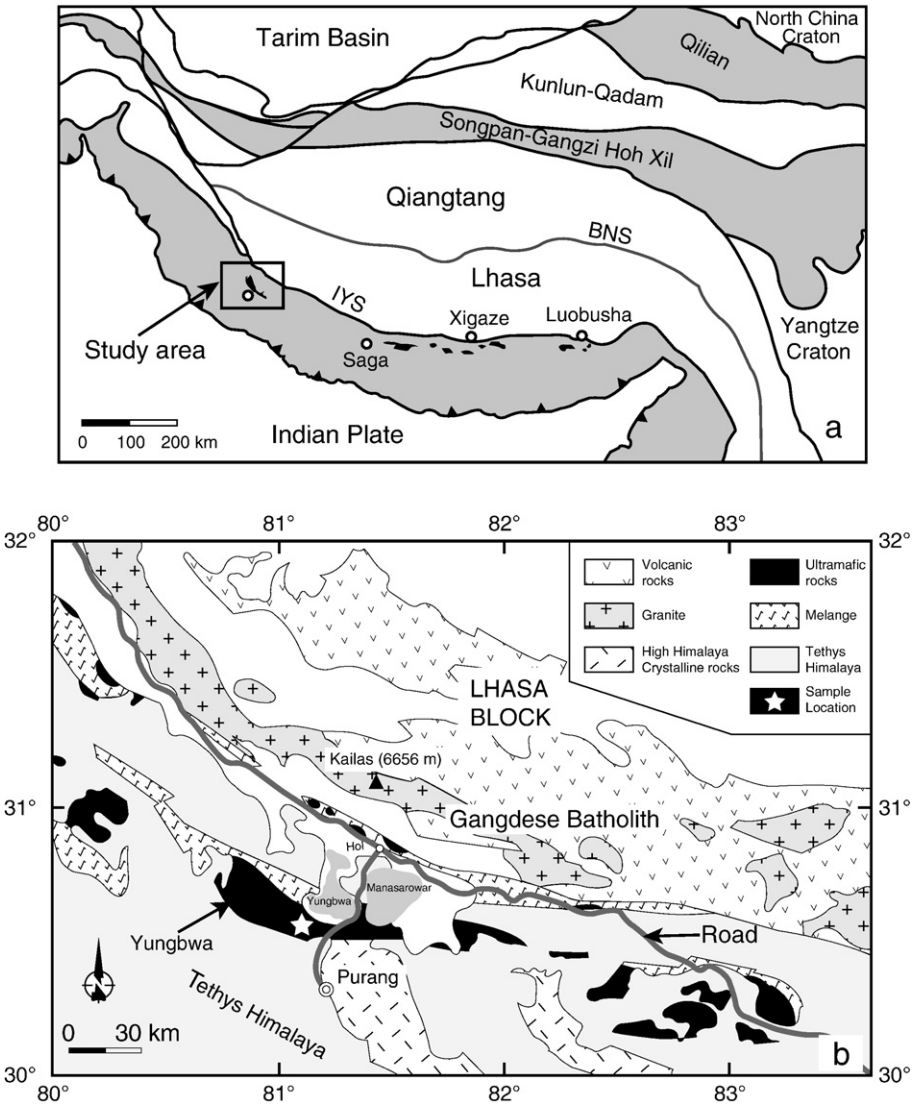

Fig. 1. (a) Sketch map of the Tibetan Plateau showing major tectonic units. The Tibetan Plateau is composed of several terranes, separated by well-defined sutures. The Indus–Yarlung Zangbo Suture is the southernmost of these, separating the Lhasa block of the Eurasian plate from the Indian plate to the south. BNS = Bagong- Nujiang Suture; IYS = Indus–Yarlung Zangbo Suture. (b) More detailed geological map of the western segment of the IYS, showing the location of the Yungbwa ophiolite.

length:width ratios of 3:1 to 8:1, defining a strong foliation. They commonly have irregular to curved margins and contain wide kink bands. However, olivine neoblasts are also present and these commonly display sharp margins and have orientations similar to the porphyroclasts. Both orthopyroxene and clinopyroxene occur as isolated and rounded porphyroclasts and locally define elongate shapes with irregular and diffuse boundaries within the olivine-rich matrix. They are oriented sub-parallel to the main foliation (Fig. 2a) and commonly display deformed cleavages and contain exsolution lamellae, that tend to be coarser and more diffuse in clinopyroxene (Fig. 2b). The orthopyroxene porphyroclasts have lobate boundaries and may contain clinopyroxene inclusions (Fig. 2c). Newly recrystallised pyroxene neoblasts also occur and commonly do not show deformation or exsolution. Spinel is generally small and round in shape and occurs disseminated among orthopyroxene and olivine, however, a few large grains (0.2–1 mm) with a "holly-leaf" shape can also be observed (Fig. 2d).

Both amphibole and plagioclase are unevenly distributed in all three samples. Amphibole blebs can also be observed within orthopyroxene porphyroclasts (Fig. 2c). Plagioclase (10–500 μm in size) is anhedral and commonly replaces clinopyroxene and orthopyroxene (Fig. 3a). Inclusions of both clinopyroxene and orthopyroxene grains are locally observed within the plagioclase (Fig. 3b). Amphibole tends to be interstitial to pyroxene and olivine in many cases (Fig. 3a), but it also occurs as blebs at the rims of orthopyroxene (Fig. 3c), or within orthopyroxene, where it is aligned with the clinopyroxene exsolution lamellae (Fig. 3d). Lamellae of amphibole and clinopyroxene have previously been observed in mantle wedge xenoliths from Papua New Guinea (Franz et al., 2002).

4. Analytical methods

4.1. Whole-rock and major element mineral chemistry

Whole-rock major element compositions were determined by X-ray fluorescence (XRF) with analytical uncertainties ranging from 1% to 3% at the Institute of Geology and Geophysics, Chinese Academy of Sciences (IGGCAS), Beijing.

Major elements in clinopyroxene, orthopyroxene and plagioclase were measured using a JEOL JXA-8200 electron microscope with an accelerating potential of 15 kV and sample current of 12 nA at the Max-Planck Instiute for Chemistry, Mainz. Major elements in olivine were also measured on the same instrument but with an accelerating potential of 20 kV and sample current of 300 nA, as described by Sobolev et al. (2007). Major elements in amphibole were determined using a JEOL JXA-8100 electron microprobe with an accelerating potential of 15 kV and sample current of 10 nA at IGGCAS.

4.2. Clinopyroxene trace element analyses

Trace elements in clinopyroxene were analyzed using a laser ablation inductively-coupled mass spectrometer (LA-ICP-MS) at IGGCAS. The laser ablation ICP-MS system consists of a Lambda Physik LPX 120I pulsed ArF excimer laser coupled to an Agilent 7500 ICP-MS. Isotopes were measured in peak-hopping mode. A glass standard, NIST 610, was used as an external calibration standard. For most of the trace elements, the MPI-DING reference material GOR-132G standard was used as a monitoring standard. Calcium (^{43}Ca) was selected as an internal standard. The CaO contents of NIST 610 and

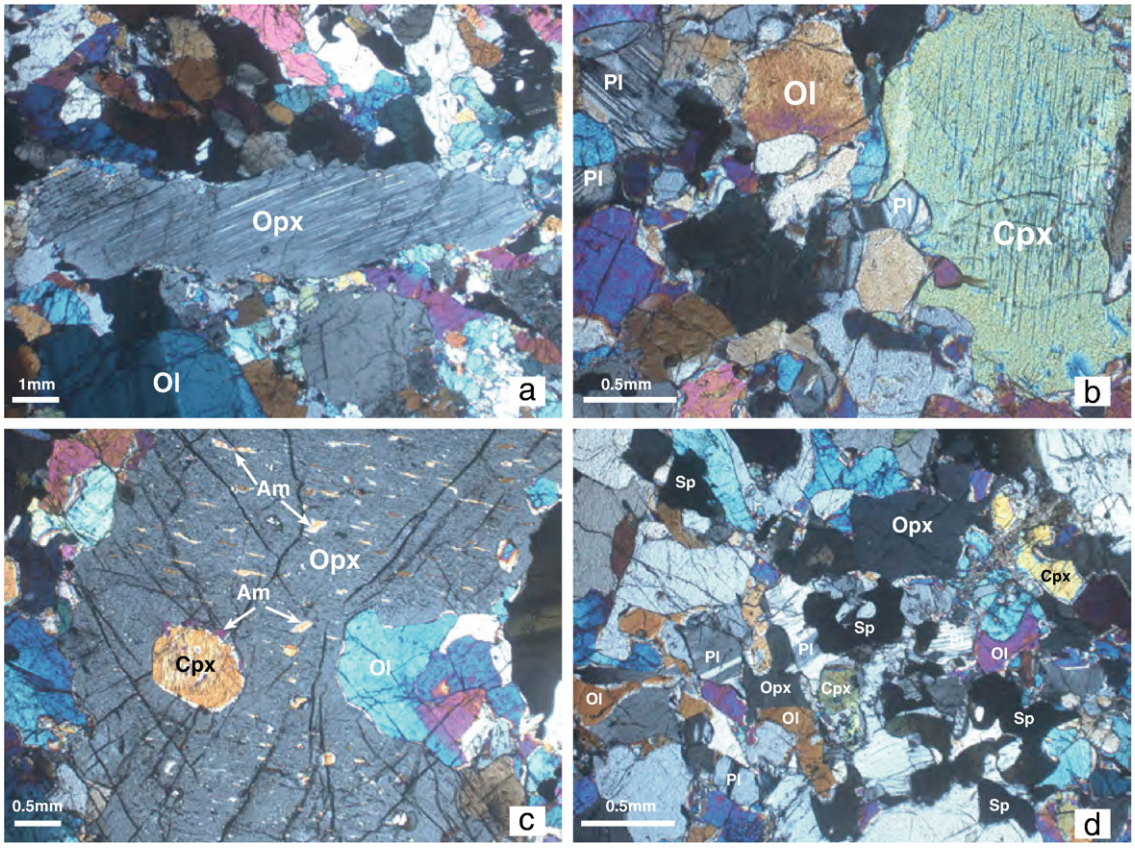

Fig. 2. Photomicrographs showing textures in plagioclase peridotites. (a) Elongated orthopyroxene (Opx) porphyroclast with irregular and diffuse boundaries against the interstitial olivine (Ol) matrix. (b) Clinopyroxene (Cpx) porphyroclast with coarse exsolution lamellae and embayed by plagioclase (Pl). (c) Orthopyroxene porphyroclast with exsolution lamellae partly replaced by olivine (Ol). It also contains clinopyroxene (Cpx) inclusions and amphibole (Am) blebs, which are aligned with the clinopyroxene lamellae. (d) Small crystals of spinel (Sp) disseminated among orthopyroxene (Opx), olivine (Ol) and plagioclase (Pl).

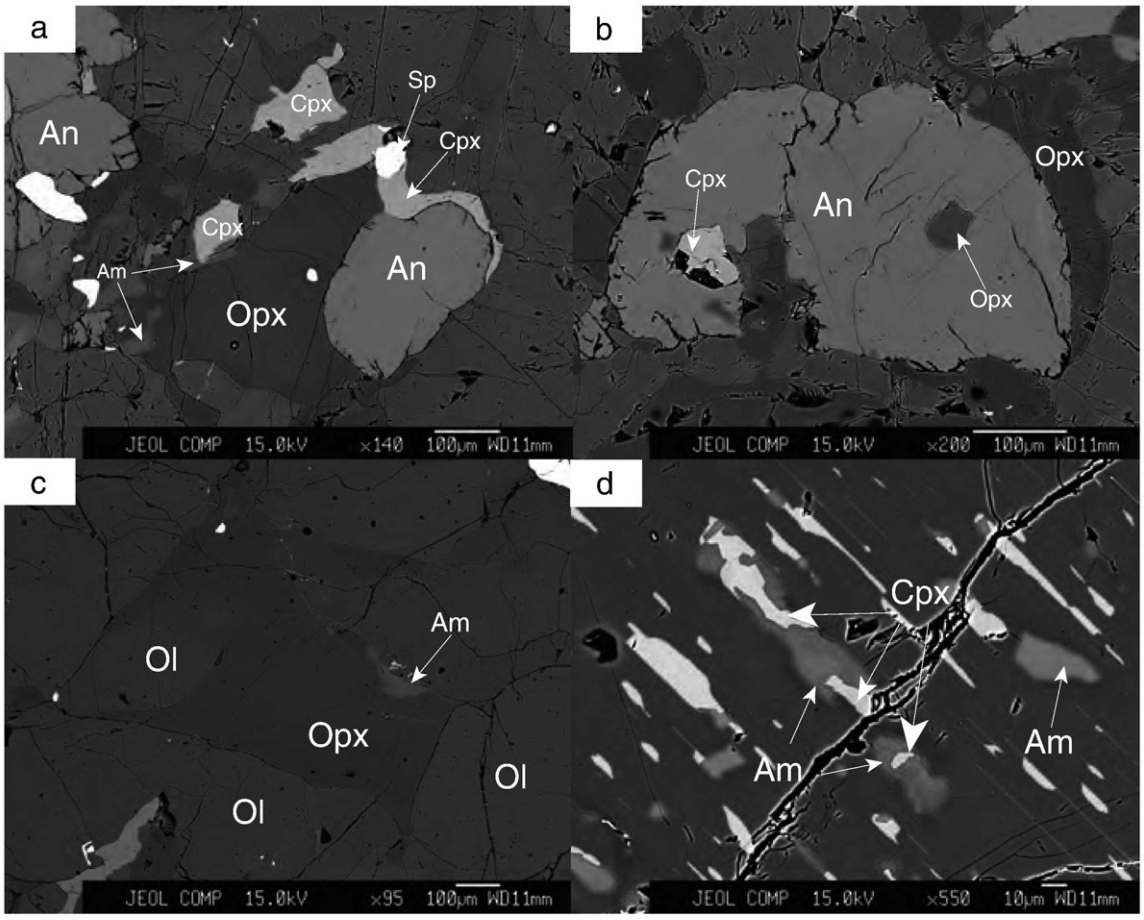

Fig. 3. Back-scattered electron (BSE) images of reaction textures in plagioclase peridotites. (a) Homogeneous anorthite (An) crystal is interstitial between clinopyroxene (Cpx) and orthopyroxene (Opx), whereas amphibole (Am) occurs along grain boundaries of both clinopyroxene and orthopyroxene. (b) Inclusions of clinopyroxene (Cpx) and orthopyroxene (Opx) in anorthite (An). (c) Amphibole (Am) replaces orthopyroxene (Opx) at the rim of an orthopyroxene (Opx) porphyroclast; olivine (Ol) is also present. (d) Lamellae of clinopyroxene (Cpx) and amphibole (Am) within an orthopyroxene porphyroclast, indicating that amphibole formed at the expense of clinopyroxene. The growth of amphibole occurred after the exsolution lamellae were formed.

GOR-132G used in the calculation are 11.5 wt.% and 8.45 wt.%, respectively. Reference values of NIST 610 and GOR-132G were from GeoREM (http://georem.mpch-mainz.gwdg.de). The data were reduced using the GLITTER 4.0 developed by GEMOC, Macquarie University (van Achterbergh et al., 2001).

5. Geochemical data

5.1. Whole-rock chemistry

Whole-rock major element analyses of the Yungbwa peridotites are listed in Table 1. All three samples have very low LOI (loss on ignition) values (<0.5 wt.%), consistent with their fresh status. Low contents of Al_2O_3 (1.52–2.07 wt.%) and CaO (1.49–1.69 wt.%) support their refractory nature. Compared to abyssal plagioclase peridotites, the Yungbwa plagioclase peridotites contain unusually low Na_2O (0.02–0.07 wt.%) and TiO_2 (0.02–0.03 wt.%).

5.2. Mineral chemistry

5.2.1. Olivine

Major element compositions of olivine are listed in Table 2. Olivine from the three samples has forsterite contents [Fo = 100 × molar Mg/(Mg + Fe)] of 90–91, with a NiO content of 0.382–0.392 wt.% and CaO content of ca. 0.02 wt.%.

5.2.2. Spinel

Consistent with spinel previously described in plagioclase-bearing peridotites (Dick, 1989; Seyler and Bonatti, 1997), spinel in the Yungbwa plagioclase peridotites also has heterogeneous compositions

Table 1
Whole-rock major element compositions of the Yungbwa plagioclase peridotites.

Sample	SiO_2	Al_2O_3	TiO_2	FeO	MnO	MgO	CaO	Na_2O	K_2O	P_2O_5	LOI	Total	Mg#
GHP-88	45.27	1.80	0.03	8.21	0.12	42.63	1.69	0.05	0.01	0.01	0.02	99.83	0.90
GHP-89	45.56	2.07	0.02	8.17	0.12	42.43	1.59	0.07	0.01	0.01	0.22	100.26	0.90
GHP-L2	45.64	1.52	0.02	7.95	0.12	43.21	1.49	0.02	0.01	0.00	0.19	100.18	0.91

Mg# = molar Mg/(Mg + Fe).

Table 2
Major element compositions of olivines, orthopyroxenes and clinopyroxenes in Yungbwa plagioclase peridotites.

Olivine													
		n	SiO_2	TiO_2	Al_2O_3	CaO	FeO	MnO	MgO	NiO	CoO	Cr_2O_3	Total	Mg#
GHP-88	Average	8	40.813	0.002	0.000	0.016	9.505	0.131	49.460	0.382	0.041	0.002	100.35	0.90
	sd		0.059	0.001	0.000	0.003	0.071	0.003	0.069	0.006	0.001	0.001	0.09	0.00
GHP-89	Average	9	40.694	0.002	0.000	0.020	9.564	0.132	49.502	0.385	0.042	0.001	100.34	0.90
	sd		0.088	0.001	0.000	0.005	0.063	0.002	0.129	0.005	0.001	0.001	0.18	0.00
GHP-L2	Average	8	40.610	0.001	0.000	0.017	9.203	0.134	49.512	0.392	0.041	0.001	99.91	0.91
	sd		0.043	0.001	0.000	0.004	0.054	0.002	0.063	0.003	0.001	0.001	0.05	0.00

Orthopyroxene													
		n	SiO_2	TiO_2	Al_2O_3	Cr_2O_3	FeO	MnO	MgO	CaO	Na_2O	K_2O	Total	Mg#
GHP-88-Pc	Average	8	55.28	0.06	3.02	0.79	6.47	0.13	33.28	1.11	0.02	0.01	100.15	0.90
	sd		0.25	0.02	0.19	0.07	0.09	0.02	0.45	0.52	0.02	0.00	0.17	0.00
GHP-88-Pr	Average	8	55.72	0.05	2.87	0.44	6.55	0.14	33.23	0.96	0.01	0.01	99.98	0.90
	sd		1.17	0.01	2.17	0.12	0.44	0.03	2.27	1.20	0.01	0.01	0.62	0.00
GHP-88-S	Average	8	56.38	0.06	1.69	0.33	6.68	0.14	34.32	0.56	0.01	0.00	100.18	0.90
	sd		0.61	0.02	0.55	0.17	0.08	0.02	0.51	0.23	0.01	0.01	0.39	0.00
GHP-89-Pc	Average	8	55.42	0.07	2.90	0.75	6.52	0.15	33.57	0.92	0.01	0.00	100.31	0.90
	sd		0.33	0.02	0.39	0.11	0.11	0.02	0.35	0.36	0.02	0.00	0.34	0.00
GHP-89-Pr	Average	8	56.73	0.05	1.35	0.21	6.68	0.15	34.67	0.39	0.01	0.00	100.24	0.90
	sd		0.36	0.03	0.33	0.05	0.16	0.03	0.45	0.12	0.01	0.01	0.27	0.00
GHP-89-S	Average	8	56.60	0.06	1.51	0.28	6.72	0.13	34.67	0.46	0.01	0.01	100.46	0.90
	sd		0.32	0.02	0.37	0.13	0.11	0.03	0.30	0.08	0.01	0.01	0.33	0.00
GHP-L2-Pc	Average	8	55.15	0.02	3.47	0.86	6.34	0.15	33.49	0.86	0.02	0.00	100.35	0.90
	sd		0.19	0.01	0.08	0.05	0.13	0.02	0.41	0.55	0.02	0.00	0.27	0.00
GHP-L2-Pr	Average	8	56.25	0.02	1.94	0.45	6.43	0.16	34.55	0.46	0.02	0.00	100.28	0.91
	sd		0.62	0.02	0.40	0.17	0.21	0.02	0.60	0.07	0.02	0.01	0.44	0.00
GHP-L2-S	Average	8	56.65	0.02	1.35	0.23	6.42	0.14	34.60	0.41	0.01	0.00	99.85	0.91
	sd		0.60	0.01	0.44	0.13	0.07	0.02	0.46	0.12	0.01	0.01	0.43	0.00

Clinopyroxene													
		n	SiO_2	TiO_2	Al_2O_3	Cr_2O_3	FeO	MnO	MgO	CaO	Na_2O	K_2O	Total	Mg#
GHP-88-Pc	Average	12	52.20	0.15	3.04	0.98	2.60	0.08	17.20	23.14	0.07	0.01	99.47	0.92
	sd		0.30	0.03	0.21	0.10	0.12	0.02	0.39	0.67	0.02	0.01	0.28	0.00
GHP-88-Pr	Average	12	52.85	0.16	2.37	0.68	2.31	0.06	17.18	23.91	0.06	0.01	99.59	0.93
	sd		0.36	0.05	0.32	0.13	0.15	0.02	0.33	0.27	0.03	0.01	0.38	0.00
GHP-88-S	Average	12	52.79	0.14	2.36	0.64	2.42	0.08	17.38	23.67	0.06	0.01	99.54	0.93
	sd		0.30	0.03	0.36	0.15	0.17	0.02	0.31	0.51	0.02	0.01	0.41	0.00
GHP-89-Pc	Average	12	52.52	0.16	2.82	0.91	2.62	0.08	17.43	23.22	0.08	0.01	99.84	0.92
	sd		0.22	0.02	0.27	0.11	0.12	0.03	0.37	0.59	0.03	0.01	0.43	0.00
GHP-89-Pr	Average	12	53.07	0.16	2.23	0.65	2.22	0.07	18.02	22.77	0.07	0.00	99.27	0.94
	sd		0.69	0.03	0.24	0.12	0.14	0.02	1.13	2.32	0.04	0.00	0.57	0.00
GHP-89-S	Average	12	52.82	0.15	2.40	0.68	2.48	0.08	17.41	23.55	0.06	0.01	99.64	0.93
	sd		0.31	0.04	0.31	0.13	0.11	0.03	0.24	0.34	0.02	0.01	0.34	0.00
GHP-L2-Pc	Average	12	52.45	0.07	2.70	0.90	2.50	0.09	17.39	23.15	0.07	0.01	99.33	0.93
	sd		0.19	0.04	0.23	0.09	0.10	0.03	0.27	0.35	0.03	0.01	0.22	0.00
GHP-L2-Pr	Average	12	53.45	0.06	1.47	0.39	2.04	0.07	17.85	23.88	0.05	0.00	99.28	0.94
	sd		0.46	0.03	0.56	0.21	0.12	0.03	0.45	0.32	0.02	0.01	0.41	0.00
GHP-L2-S	Average	12	53.15	0.07	1.86	0.55	2.19	0.07	17.59	23.78	0.06	0.01	99.32	0.93
	sd		0.57	0.03	0.55	0.20	0.16	0.02	0.37	0.32	0.02	0.01	0.41	0.00

sd = standard deviation.
Pc = porphyroclast core; Pr = porphyroclast rim; S = small neoblast.

(EA Table 1). The Cr# [= molar Cr/(Cr + Al)] varies from 0.38 to 0.44 for GHP-88, 0.31 to 0.43 for GHP-89 and 0.22 to 0.43 for GHP-L2. The TiO_2 content (<0.2) is significantly lower than spinel reported from plagioclase-bearing abyssal peridotites (Fig. 4).

5.2.3. Orthopyroxene

Major element compositions of both orthopyroxene and clinopyroxene are listed in Table 2. Core-rim and large-to-small orthopyroxene grains have a compositional variation that defines a unique trend at the sample scale. Aluminium, Cr and Ca decrease, whereas Si and Mg increase, from core to rim and from large to small grains (Fig. 5a, b). These variations result in a slight increase of Mg# [= molar Mg/(Mg + Fe)] and a slight decrease in Cr/Al ratio and wollastonite content from core to rim.

Mg# of orthopyroxene varies from 0.90 to 0.91. The ratios of the olivine/orthopyroxene Mg# in all three samples are close to unity, suggesting equilibrium under high-temperature mantle conditions. The orthopyroxene porphyroclastic cores have Al_2O_3 contents of 2.90 wt.% to 3.47 wt.% and CaO contents of 0.86 wt.% to 1.11 wt.%.

5.2.4. Clinopyroxene

Clinopyroxene in the Yungbwa samples is chromian diopside containing ~0.9 wt.% Cr_2O_3 and having a high Mg# (0.92–0.93). The grains have low contents of both TiO_2 (0.07–0.16 wt.%) and Na_2O (0.07–0.08 wt.%). They also display consistent core-rim and large-to-small grain compositional variations, similar to those displayed by orthopyroxenes, i.e., Al, Cr and Ca decrease but Si and Mg increase from core to rim and from porphyroclasts to neoblasts. The cores of the clinopyroxene porphyroclasts have Al_2O_3 contents ranging from 2.7 wt.% to 3.04 wt.%, supporting the refractory nature of these samples.

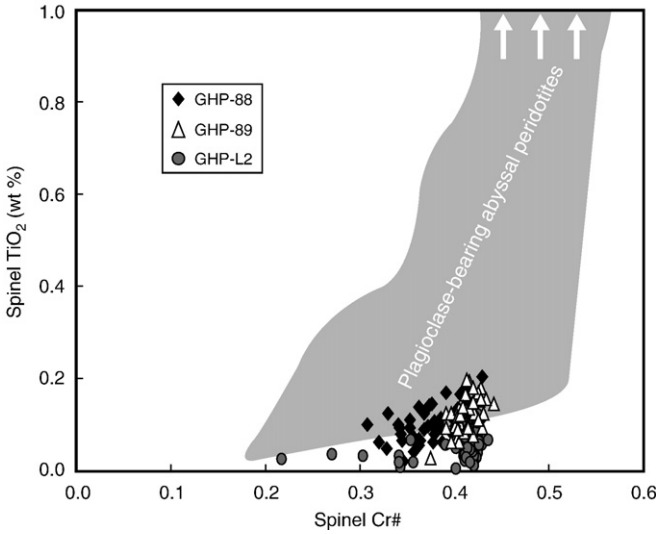

Fig. 4. Plot of TiO_2 content versus Cr# of spinels in the Yungbwa plagioclase peridotites. The spinels in the Yungbwa plagioclase peridotites have much lower TiO_2 contents relative to those in plagioclase-bearing abyssal peridotites. Field of plagioclase-bearing abyssal peridotites is from Hellebrand et al. (2002b).

Table 3
Trace element compositions of clinopyroxenes of the Yungbwa plagioclase peridotites.

	GHP-88	GHP-89	GHP-L2
Ti	882	913	477
Sr	0.43	0.47	0.28
Y	6.04	5.95	5.77
Zr	0.28	0.24	0.65
Nb	0.02	0.03	0.03
La	0.02	0.02	0.08
Ce	0.06	0.06	0.17
Pr	0.01	0.01	0.02
Nd	0.04	0.04	0.08
Sm	0.06	0.06	0.07
Eu	0.03	0.03	0.03
Gd	0.34	0.34	0.32
Tb	0.10	0.10	0.10
Dy	0.98	0.95	0.91
Ho	0.25	0.25	0.24
Er	0.78	0.76	0.78
Tm	0.12	0.11	0.11
Yb	0.78	0.74	0.79
Lu	0.11	0.11	0.11
Hf	0.03	0.03	0.04

The trace element compositions of clinopyroxene are listed in Table 3. Clinopyroxene from all three samples displays similar rare earth element (REE) patterns with depletion from heavy rare earth elements (HREE) to middle rare earth elements (MREE) [$(Sm/Yb)_N = 0.09–0.1$], but flat for the light rare earth elements (LREE) [$(La/Nd)_N = 0.97–1.76$] (Fig. 6a). The analyses reveal slight negative Zr and Ti anomalies, which

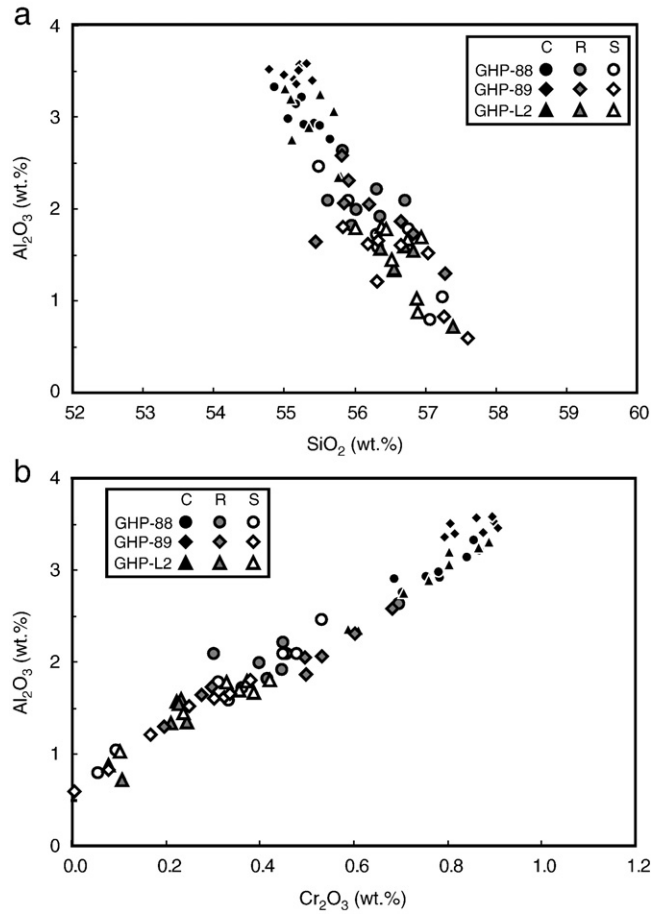

Fig. 5. Composition of orthopyroxene. (a) Al_2O_3 (wt.%) vs SiO_2 (wt.%), showing the decrease of Al_2O_3 content from the core to the rim in the large porphyroblasts along with the increase of SiO_2. (b) Al_2O_3 (wt.%) vs Cr_2O_3 (wt.%), indicating that the contents of both oxides decrease from the core to the rim in the large porphyroblasts. Note that the small neoblasts have compositions similar to the rim of the large porphyroblasts. C = core, R = rim, and S = small neoblast.

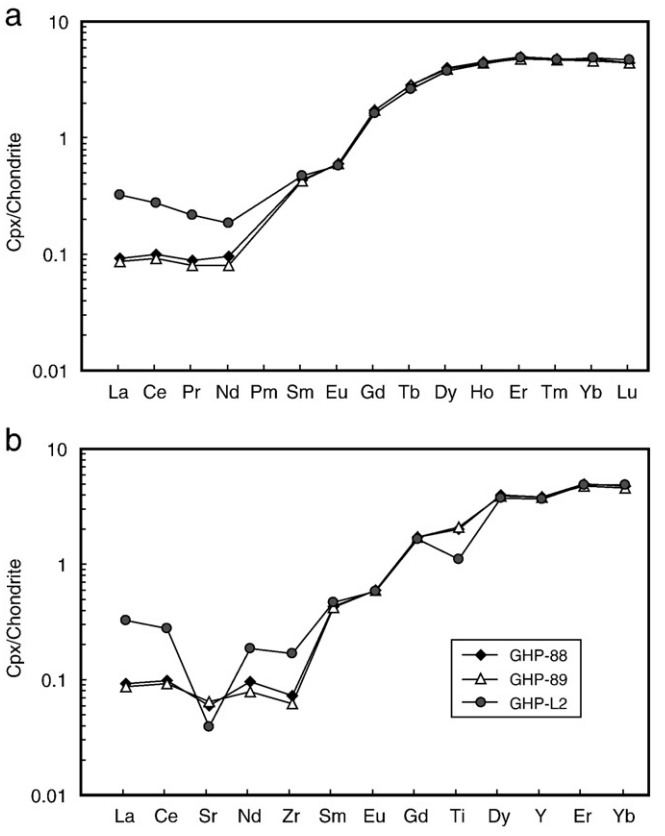

Fig. 6. Diagrams of chondrite-normalized (a) REE and (b) trace element patterns of clinopyroxene in the Yungbwa peridotites. GHP-88 and -89 have similar patterns in both REE and trace elements, whereas GHP-L2 has higher LREE contents. Clinopyroxenes from all samples show negative Zr and Ti anomalies. Negative Eu and Sr anomalies reflect the segregation of plagioclase during melt impregnation. Chondrite-normalized values are from Anders and Grevesse (1989).

are typical characteristics of clinopyroxene in mantle peridotites. Small negative Eu and Sr anomalies in the clinopyroxene might result from the formation of plagioclase. In particular, clinopyroxene in sample GHP-L2 displays negative Sr and Ti anomalies stronger than those in both GHP-88 and -89 (Fig. 6b).

5.2.5. Plagioclase

Plagioclase occurs in all samples and has a homogeneous composition without zoning (EA Table 2). The grains have high CaO contents (19.5–20.5 wt.%) but very low contents of both Na_2O (<0.25 wt.%) and K_2O (<0.05 wt.%), giving the very high anorthite contents (An_{98-99}).

5.2.6. Amphibole

Amphibole in all samples has a pargasitic composition (EA Table 3), belonging to the calcic amphibole group (Leake et al., 1997). The grains are highly magnesian with Mg# of 0.91–0.95, and have variable contents of both Al_2O_3 and Cr_2O_3. Furthermore, they contain very low abundances of both Na_2O (<0.9 wt.%) and TiO_2 (0.08–0.66 wt.%).

6. Discussion

6.1. Origin of the pargasitic amphibole

In serpentinised abyssal peridotites, amphibole is commonly associated with altered minerals such as serpentine and talc (e.g., Cannat and Seyler, 1995) and, if formed during seawater alteration, generally has a tremolitic composition. The Yungbwa peridotites are fresh and little serpentine and talc have been observed under the microscope, which is also supported by their very low LOI. Amphibole occurs as either blebs at the rims of fresh orthopyroxene or as patches in alignment with the clinopyroxene exsolution lamellae within orthopyroxene. These textures suggest that they were formed by reaction with fluids or melts, during which both clinopyroxene and orthopyroxene were replaced by amphibole. Furthermore, the pargasitic composition of amphibole in the Yungbwa peridotites is different from normal alteration-related amphiboles. Pargasitic amphiboles have been commonly found in modally metasomatised mantle peridotites, occasionally with other volatile-bearing minerals, e.g., phlogopite (Coltorti et al. (2007) and reference therein). There is a general consensus that the presence of these minerals is related to the percolation and reaction of metasomatising agents with the originally 'dry' peridotites (Ionov et al., 1997). In addition, clinopyroxene in the Yungbwa peridotites has flat LREE patterns, indicating that they were metasomatised by late melts after partial melting. Therefore, all these evidence suggest that the amphiboles discovered in the Yungbwa peridotites resulted from fluid/melt metasomatism rather than seawater alteration. On the other hand, replacement textures displayed by the amphiboles suggest that the metasomatic processes occurred after the formation of the exsolution lamellae in the orthopyroxenes. This may imply that the hydrous melts were introduced into the Yungbwa peridotites at shallow lithospheric depths (Franz et al., 2002). The stability of the plagioclase in these samples indicates that the depth should be shallower than 35 km (Green and Hibberson, 1970).

It has been suggested that the chemical composition of amphibole can fingerprint the nature of the metasomatising agents introduced into the mantle peridotites (Coltorti et al., 2007). Previous studies have demonstrated that amphibole can show the signature of the metasomatising fluids or melts (Ionov and Hofmann, 1995; Coltorti et al., 2004). For example, amphiboles in mantle xenoliths from subduction zone settings generally have lower HFSE (e.g., Nb) and Ti contents relative to those occurring in xenoliths from intraplate settings (Coltorti et al., 2007). Amphiboles in the Yungbwa peridotites have not been analyzed for trace elements, since their size is too small for laser ablation analysis. However, they contain low Ti contents (0.06–0.66 wt.%), which are close to amphiboles identified in mantle wedge peridotites but much lower than those found in mantle xenoliths from intraplate settings (Coltorti et al., 2007). This implies that the agents metasomatising the Yungbwa peridotites have arc affinities.

6.2. Formation of anorthitic plagioclase in the Yungbwa peridotites

Anorthitic plagioclase has been rarely reported in mantle peridotites (Hamlyn and Bonatti, 1980; Arai, 1991; Cannat and Seyler, 1995; Rampone et al., 1997; Franz et al., 2002). The mechanism by which anorthitic plagioclase can form in mantle peridotites is still unclear. Its origin has been explained either by spinel breakdown (Hamlyn and Bonatti, 1980; Cannat and Seyler, 1995) or by melt metasomatism (Arai, 1991; Rampone et al., 1997). Plagioclase with a composition of almost pure anorthite (An~98), together with pargasitic amphibole, have previously been reported in mantle wedge xenoliths from Papua New Guinea (Franz et al., 2002). These authors explained that such a mineral assemblage was produced by the reaction of hydrous arc magmas with spinel peridotites. Formation of pargasitic amphibole indicates that the Yungbwa peridotites were invaded by exotic hydrous melts. The anorthitic plagioclases also display textures supporting their formation at the expense of both clinopyroxene and orthopyroxene (Fig. 3a, b). This evidence eliminates the possibility of the formation of anorthitic plagioclase in the Yungbwa peridotites by spinel breakdown in a closed system, but does support its formation through the process of melt metasomatism.

It has been widely documented that the impregnating melts can differentiate to plagioclase ± clinopyroxene ± orthopyroxene blebs when trapped in peridotites (e.g., Dick, 1989; Rampone et al., 1997; Dijkstra et al., 2003; Rampone et al., 2008). Such blebs represent a cooling stage when the melt becomes saturated in these minerals (Dijkstra et al., 2003). The hydrous melts commonly react with the host peridotite after impregnation. Textures displayed by amphibole in the Yungbwa peridotite reflect that they replaced both orthopyroxenes (Fig. 3c) and clinopyroxenes (Fig. 3d), which suggest that both pyroxenes were partially dissolved by the hydrous melt. Locally, plagioclase displays embayment textures where it partly corrodes the clinopyroxene porphyroclasts (Fig. 2b). However, it is more commonly rimmed by irregular clinopyroxene and orthopyroxene at their rims (Fig. 3a). Orthopyroxene inclusions within plagioclase can locally be observed in the Yungbwa samples (Fig. 3b). All these textures substantiate that anorthitic plagioclase in the Yungbwa peridotites was produced at the expense of both clinopyroxene and orthopyroxene. Besides amphibole and plagioclase, olivine was also introduced from the metasomatising melt into the peridotites. The embayment of undeformed olivine into orthopyroxene with exsolution lamellae (see Fig. 2c) reflects a reactive porous flow process in the Yungbwa peridotites, during which orthopyroxene was resorbed and replaced by olivine (Piccardo, 2003; Rampone et al., 2008). Furthermore, the occurrence of Al-poor rims in the spinels also indicates that they were affected by the hydrous melt. Therefore, the formation of amphibole and plagioclase in the Yungbwa peridotites could be represented by the reaction: clinopyroxene + orthopyroxene + spinel + melt → olivine + amphibole + plagioclase.

During reaction with peridotite, the hydrous melt dissolved and transferred soluble components from the peridotites. Textures indicate that both orthopyroxene and clinopyroxene were dissolved whereas olivine was precipitated, which suggests that the metasomatic melt was SiO_2-undersaturated. This may be attributed to the hydrous state of the melt, because water would increase the SiO_2 content of an olivine-saturated melt (Kelemen, 1995). Furthermore, the dissolution of pyroxene and crystallization of olivine observed in the Yungbwa peridotites mimic the process proposed to explain the formation of high-Mg andesites through the reaction of hydrous melt

with mantle peridotites (Kelemen, 1995). When the hydrous melt became saturated in dissolved components, secondary metasomatic minerals tend to be precipitated (McInnes et al., 2001). This finally results in the precipitation of clinopyroxene and orthopyroxene neoblasts. Both clinopyroxene and orthopyroxene neoblasts with higher SiO_2 and lower Al_2O_3 contents than the primary pyroxene porphyroclasts are evident in the Yungbwa samples (Fig. 5).

6.3. Compositional features of the impregnating melts

Formation of metasomatic minerals could provide information about the composition of the impregnated melt (Ionov and Hofmann, 1995; Vannucci et al., 1995; Coltorti et al., 2004; Coltorti et al., 2007). Plagioclase peridotites formed through melt impregnation generally have higher contents of both Na and Ti than the residual spinel peridotites (Dick, 1989). The Yungbwa plagioclase peridotites, however, have remarkably low concentrations of both Na and Ti (0.02–0.07 wt.% and ca. 0.03 wt.%, respectively) relative to plagioclase-bearing peridotites recovered from the seafloor (see Fig. 4). On the one hand, low contents of both elements can result from large degrees of partial melting in these samples, as evidenced by their pyroxene compositions, e.g., low Al_2O_3 and HREE contents in clinopyroxenes. On the other hand, this might also be due to the severe depletion of both Na and Ti in the impregnating melts.

Although rare in mantle peridotites (Hamlyn and Bonatti, 1980; Arai, 1991; Cannat and Seyler, 1995; Rampone et al., 1997; Franz et al., 2002), anorthitic plagioclase occurs widely in lavas and plutonic rocks from both the mid-ocean ridge (Sinton et al., 1993; Johnson et al., 1995; Nielsen et al., 1995; Dick and Natland, 1996) and convergent margin settings (Arculus and Wills, 1980; Falloon and Green, 1986; Danyushevsky et al., 1997). It has been demonstrated by previous experimental studies that the anorthite content of plagioclase crystallizing from magma is mainly controlled by the Al/Si and Ca/Na ratios and water contents of the melt (Johannes, 1989; Sisson and Grove, 1993; Panjasawatwong et al., 1995). Therefore, anorthitic plagioclase can crystallize from either water-saturated melts or refractory magmas with high Al/Si and Ca/Na ratios. The hydrous melts that impregnated the Yungbwa peridotites were unlikely to be water-saturated. Therefore, plagioclases up to An_{99} in the Yungbwa peridotites might reflect that the metasomatising hydrous melts were also refractory with high Ca/Na and Al/Si ratios. Although lavas with such refractory compositions have been rarely reported, their existence is supported by melt inclusions with ultra-depleted compositions in olivine crystals in arc lavas (Falloon and Green, 1986), which could be produced by partial melting of already depleted peridotitic source under 'wet' conditions.

The low Ti content in spinel implies the depletion of Ti in the metasomatising melt. In plagioclase peridotites, Ti content of spinels reflects the nature or volume of the impregnating melts, rather than the primary signatures of the host peridotites (Cannat et al., 1990). Impregnating melts are generally richer in Ti relative to residual peridotites, and thus, spinel equilibrating with such melts should have higher Ti contents (Pearce et al., 2000). Compared to those in seafloor plagioclase peridotites, however, spinels in the Yungbwa peridotites have much lower Ti contents (<0.2 wt.%; Fig. 4), which suggests that the hydrous melts metasomatising the Yungbwa peridotites contained less Ti than mid-ocean ridge basalt (MORB). Furthermore, depletion of Ti in the metasomatic melts is also supported by the low Ti content of the pargasitic amphibole. It has been suggested that the Ti content of metasomatic amphibole is highly dependent on the composition of the metasomatic agent (Coltorti et al., 2007). For example, lower Ti contents of amphibole in mantle wedge peridotites compared to those in mantle xenoliths from intraplate settings have been attributed to the lower Ti content in subduction zone magmas relative to intraplate magmas (Coltorti et al., 2007). Titanium contents of amphiboles in the Yungbwa peridotites are close to amphiboles identified in mantle wedge peridotites, but much lower than those in mantle xenoliths from intraplate settings.

Clinopyroxene in plagioclase-bearing ophiolitic and abyssal peridotites is generally depleted in LREE, reflecting the depleted nature of the impregnating melt (Rampone et al., 1997; Dijkstra et al., 2003). Percolation and interaction with depleted melt have been documented in many ophiolitic and abyssal peridotites (Rampone et al., 1997; Batanova and Sobolev, 2000; Seyler et al., 2001; Dijkstra et al., 2003; Piccardo et al., 2007; Rampone et al., 2008), and their origin has been explained by different hypotheses, e.g., reaction with depleted lithospheric mantle or partial melting of shallow refractory peridotite. On the contrary, clinopyroxene in the Yungbwa samples displays either enriched (GHP-L2) or flat LREE (GHP-88 and -89) patterns, which reflects the enrichment of LREE in the metasomatising melt. Similar patterns have been reported in plagioclase-bearing mantle xenoliths from the Tabar–Lihir–Tanga–Feni island arc in Papua New Guinea, which have been subjected to pervasive reaction with arc magmas (Grégoire et al., 2001; Franz et al., 2002).

Although the exact composition of the metasomatic melt cannot be quantitatively determined, constraints from the known composition of the metasomatic minerals require that the hydrous melt was highly depleted in Na and Ti relative to MORB, but more enriched in LREE than MREE and HREE. These characteristics are quite different from MORB (Metcalf and Shervais, 2008), arguing against the evolution of the Yungbwa ophiolite solely in a mid-ocean ridge setting, as previously proposed (Miller et al., 2003). On the contrary, such geochemical characteristics show affinities to island arc magmas, a feature that could be achieved through hydrous partial melting of an already depleted mantle source within a subduction zone.

6.4. Tectonic evolution of the Yungbwa ophiolite

It has been demonstrated that both supra-subduction and abyssal peridotites can be juxtaposed in the same ophiolite, reflecting the fact that an ophiolite can experience a multi-stage evolution in different tectonic settings (Batanova and Sobolev, 2000; Choi et al., 2008). Similar conclusions have been arrived at by previous studies on ophiolites outcropping along the Indus–Yarlung Zangbo Suture (Zhou et al., 1996; Wang et al., 2000; Hout et al., 2002; Hébert et al., 2003; Malpas et al., 2003; Dubois-Côté et al., 2005; Zhou et al., 2005). However, the formation setting of ophiolite in the western segment of the Indus–Yarlung Zangbo Suture, e.g., Yungbwa ophiolite, is still unclear. It has been shown in a previous study that the composition of mantle peridotites in the Yungbwa ophiolite is similar to abyssal peridotites from slow-spreading mid-ocean ridges and that associated basaltic lavas and dykes also have compositions similar to N-MORB (Miller et al., 2003). This evidence led the authors to conclude that the Yungbwa ophiolite originated at a slow-spreading mid-ocean ridge.

The reaction of the Yungbwa peridotites with hydrous melts of subduction affinity provides compelling support that they underwent modification in a subduction zone setting. Juxtaposition of both abyssal and SSZ peridotites suggests that the Yungbwa ophiolite has experienced a multi-stage evolution. First, the mantle peridotites were depleted by melt extraction, probably beneath a slow-spreading ridge, during which the initial precursor of the Yungbwa ophiolite formed (Miller et al., 2003). Subsequently, these abyssal-type peridotites entered an intra-oceanic subduction zone during the closure of the Neo-Tethys Ocean. There they were metasomatised by arc magmas derived from the mantle wedge, resulting in the formation of both pargasitic amphibole and anorthitic plagioclase. Such a two-stage evolution model is consistent with previous conclusions for the Luobusha ophiolite in the eastern segment (Zhou et al., 2005), and the Xigaze ophiolite in the central segment of the Indus–Yarlung Zangbo Suture (Hébert et al., 2003; Dubois-Côté et al., 2005). Therefore, we suggest that mantle peridotites outcropping along the entire Indus–Yarlung Zangbo Suture record both the opening of the Neo-Tethys Ocean and its closure through subduction.

7. Conclusion

An unusual mineral assemblage of anorthitic plagioclase (An_{99}) and pargasitic amphiboles has been discovered in mantle peridotites from the Yungbwa ophiolite, southwestern Tibetan Plateau. The compositions of the constituent minerals in the plagioclase peridotites suggest that they were produced through melt metasomatism, during which both clinopyroxene and orthopyroxene were consumed. The composition of the metasomatising melts have been qualitatively constrained to be highly depleted in Na and Ti compared to MORB, but enriched in LREE relative to MREE and HREE, establishing their subduction zone affinity. Therefore, we propose that that the Yungbwa ophiolite has experienced a multi-stage evolution, the first stage was formation at a mid-ocean ridge and the second was the subsequent transfer to a subduction zone setting. These rocks thus record both the opening and subsequent closure of the Neo-Tethys Ocean during the collision of India with the Eurasian plate.

Acknowledgements

Financial support was provided by the National Natural Science Foundation of China (Grant No. 40873024) and the State Key Laboratory of Lithospheric Evolution, IGGCAS (Grant No. 10801130). Discussions with Al Hofmann and K. Ye helped improve the manuscript. We thank D. Kuzmin from the Max-Planck Institute for Chemistry and Q. Mao and Y.G. Ma from IGGCAS for the help with electron microprobe analysis, and L.W. Xie for the help with LA-ICP-MS analysis. We thank M.F. Zhou and another anonymous reviewer for their constructive reviews on this manuscript and A. Kerr for the editorial handling.

Appendix A. Supplementary data

Supplementary data associated with this article can be found, in the online version, at doi:10.1016/j.lithos.2009.10.008.

References

Anders, E., Grevesse, N., 1989. Abundances of the elements: meteoritic and solar. Geochimica et Cosmochimica Acta 53, 197–214.
Arai, S., 1991. The Circum-Izu Massif Peridotites, Central Japan, as Back-arc Mantle Fragments of the Izu–Bonin Arc System. In: Peters, T.E.A. (Ed.), Ophiolite Genesis and Evolution of the Oceanic Lithosphere. Ministry of Petroleum and Minerals, Sultanate of Oman, pp. 801–816. vol.
Arculus, R.J., Wills, K.J.A., 1980. The petrology of plutonic blocks and inclusions from the Lesser Antilles island arc. Journal of Petrology 21, 743–799.
Batanova, V.G., Sobolev, A.V., 2000. Compositional heterogeneity in subduction-related mantle peridotites, Troodos massif, Cyprus. Geology 28, 55–58.
Borghini, G., Rampone, E., Crispini, L., De Ferrari, R., Godard, M., 2007. Origin and emplacement of ultramafic–mafic intrusions in the Erro–Tobbio mantle peridotites (Ligurian Alps, Italy). Lithos 94, 210–229.
Cannat, M., Bideau, D., Hebert, R., 1990. Plastic-deformation and magmatic impregnation in serpentinized ultramafic rocks from the Garrett Transform-Fault (East Pacific Rise). Earth and Planetary Science Letters 101, 216–232.
Cannat, M., Seyler, M., 1995. Transform tectonics, metamorphic plagioclase and amphibolitization in ultramafic rocks of the Vema transform fault (Atlantic Ocean). Earth and Planetary Science Letters 133, 283–298.
Choi, S.H., Shervais, J.W., Mukasa, S.B., 2008. Supra-subduction and abyssal mantle peridotites of the Coast Range ophiolite, California. Contributions to Mineralogy and Petrology 156, 551–576.
Coltorti, M., Beccaluva, L., Bonadiman, C., Faccini, B., Natflos, T., 2004. Amphibole genesis via metasomatic reaction with clinopyroxene in mantle xenoliths from Victoria Land, Antarctica. Lithos 75, 115–139.
Coltorti, M., Bonadiman, C., Faccini, B., Gregoire, M., O'Reilly, S.Y., Powell, W., 2007. Amphiboles from suprasubduction and intraplate lithospheric mantle. Lithos 99, 68–84.
Constantin, M., 1999. Gabbroic intrusions and magmatic metasomatism in harzburgites from the Garrett transform fault: implications for the nature of the mantle-crust transition at fast-spreading ridges. Contributions to Mineralogy and Petrology 136, 111–130.
Danyushevsky, L.V., Carroll, M.R., Falloon, T.J., 1997. Origin of high-An plagioclase in Tongan high-Ca boninites: implications for plagioclase-melt equilibrium at low P(H_2O). The Canadian Mineralogist 35, 313–326.
Dick, H.J.B., 1989. Abyssal Peridotites, Very Slow Spreading Ridges and Ocean Ridge Magmatism. In: Saunders, A.D., Norry, M.J. (Eds.), Magmatism in the Ocean Basins: Geological Society Special Publication, London, vol. 42, pp. 71–105.
Dick, H.J.B., Natland, J.H., 1996. In: Mével, C., Gillis, K.M., Allan, J.F., Meyer, P.S. (Eds.), Late-stage melt evolution and transport in the shallow mantle beneath the East Pacific Rise: Proceedings of the Ocean Drill Program Scientific Results, vol. 147, pp. 103–134. College Station.
Dijkstra, A.H., Barth, M.G., Drury, M.R., Mason, P.R.D., Vissers, R.L.M., 2003. Diffuse porous melt flow and melt-rock reaction in the mantle lithosphere at a slow-spreading ridge: a structural petrology and LA-ICP-MS study of the Othris Peridotite Massif (Greece). Geochemistry Geophysics Geosystems 4, 24.
Dubois-Côté, V., Hébert, R., Dupuis, C., Wang, C.S., Li, Y.L., Dostal, J., 2005. Petrological and geochemical evidence for the origin of the Yarlung Zangbo ophiolites, southern Tibet. Chemical Geology 214, 265–286.
Falloon, T.J., Green, D.H., 1986. Glass inclusions in magnesian olivine phenocrysts from Tonga: evidence for highly refractory parental magmas in the Tongan arc. Earth and Planetary Science Letters 81, 95–103.
Franz, L., Becker, K.P., Kramer, W., Herzig, P.M., 2002. Metasomatic mantle xenoliths from the Bismarck microplate (Papua New Guinea): thermal evolution, geochemistry and extent of slab-induced metasomatism. Journal of Petrology 43, 315–343.
Girardeau, J., Mercier, J.-C., Wang, X.B., 1985a. Petrology of the mafic rocks of the Xigaze ophiolite, Tibet: implications for the genesis of the oceanic lithosphere. Contributions to Mineralogy and Petrology 90, 309–321.
Girardeau, J., Mercier, J.-C., Yougong, Z., 1985b. Origin of the Xigaze ophiolite, Yarlung Zangbo suture zone, southern Tibet. Tectonophysics 119, 407–433.
Girardeau, J., Mercier, J.-C., 1988. Petrology and texture of the ultramafic rocks of the Xigaze ophiolite (Tibet): constraints for mantle structure beneath slow-spreading ridges. Tectonophysics 147, 33–58.
Grégoire, M., McInnes, B.I.A., O'Reilly, S.Y., 2001. Hydrous metasomatism of oceanic sub-arc mantle, Lihir, Papua New Guinea—part 2. Trace element characteristics of slab-derived fluids. Lithos 59, 91–108.
Green, D.H., Hibberson, W.O., 1970. The instability of plagioclase in peridotite at high pressure. Lithos 3, 209–221.
Hébert, R., Huot, F., Wang, C.S., Liu, Z.F., 2003. Yarlung Zangbo Ophiolites (Southern Tibet) Revisited: Geodynamic Implication from the Mineral Record. In: Dilek, Y., Robinson, P.T. (Eds.), Ophiolites in Earth History: Geological Society Speical Publications, London, vol. 218, pp. 165–190.
Hamlyn, P.R., Bonatti, E., 1980. Petrology of mantle-derived ultramafics from the Owen Fracture Zone, northwest Indian Ocean: implications for the nature of the oceanic upper mantle. Earth and Planetary Science Letters 48, 65–79.
Hellebrand, E., Snow, J.E., Hoppe, P., Hofmann, A.W., 2002a. Garnet-field melting and late-stage refertilization in 'residual' abyssal peridotites from the Central Indian Ridge. Journal of Petrology 43, 2305–2338.
Hellebrand, E., Snow, J.E., Muhe, R., 2002b. Mantle melting beneath Gakkel Ridge (Arctic Ocean): abyssal peridotite spinel compositions. Chemical Geology 182, 227–235.
Hout, F., Hébert, R., Varfalvy, V., Beaudin, G., Wang, C.S., Liu, Z.F., Cotten, J., Dostal, J., 2002. The Beimarang mélange (southern Tibet) brings additional constraints in assessing the origin, metamorphic evolution and obduction processes of the Yarlung Zangbo ophiolite. Journal of Asian Earth Sciences 21, 307–322.
Ionov, D., Griffin, W.L., O'Reilly, S.Y., 1997. Volatile-bearing minerals and lithophile trace elements in the upper mantle. Chemical Geology 141, 153–184.
Ionov, D.A., Hofmann, A.W., 1995. Nb–Ta-rich mantle amphiboles and micas: implications for subduction-related metasomatic trace element fractionations. Earth and Planetary Science Letters 131, 341–356.
Johannes, W., 1989. Melting of plagioclase–quartz assemblages of 2 kbar water pressure. Contributions to Mineralogy and Petrology 103, 270–276.
Johnson, K.T.M., Fisk, M.R., Naslund, H.R., 1995. In: Erzinger, J., Becker, K., Dick, H.J.B., Stokking, L.B. (Eds.), Geochemical characteristics of refractory silicate melt inclusions from Leg 140 diabases: Proceeding of ODP Scientific Results, vol. 137/140, pp. 131–139. College Station, Texas.
Kelemen, P.B., 1995. Genesis of high Mg# andesites and the continental crust. Contributions to Mineralogy and Petrology 120, 1–19.
Leake, B.E., Woolley, A.R., Arps, C.E.S., 1997. Nomenclature of amphiboles. Reports of the subcommittee on amphiboles of the International Mineralogical Association Commission on new minerals and mineral names. European Journal of Mineralogy 9, 623–651.
Lundstrom, C.C., Tepley III, F.J., 2006. Investigating the origin of anorthitic plagioclase through a combination of experiments and natural observations. Journal of Volcanology and Geothermal Research 157, 202–221.
Müntener, O., Pettke, T., Desmurs, L., Meier, M., Schaltegger, M., 2004. Trace element and Nd-isotopic evidence and implications for crust–mantle relationships. Earth and Planetary Science Letters 221, 293–308.
Malpas, J., Zhou, M.F., Robinson, P.T., Reynolds, P.H., 2003. Geochemical and Geochronological Constraints on the Origin and Emplacement of the Yarlung Zangbo Ophiolite, Southern Tibet. In: Dilek, Y., Robinson, P.T. (Eds.), Ophiolites in Earth History: Geological Society Special Publications, London, vol. 218, pp. 191–206.
McInnes, B.I.A., Gregoire, M., Binns, R.A., Herzig, P.M., Hannington, M.D., 2001. Hydrous metasomatism of oceanic sub-arc mantle, Lihir, Papua New Guinea: petrology and geochemistry of fluid-metasomatised mantle wedge xenoliths. Earth and Planetary Science Letters 188, 169–183.
Metcalf, R.V., Shervais, J.W., 2008. Suprasubduction-zone Ophiolites: Is There Really an Ophiolite Conundrum? In: Wright, J.E., Shervais, J.W. (Eds.), Ophiolite, Arcs, and Batholiths: A Tribute to Cliff Hopson: The Geological Society of America Special Paper, Boulder, vol. 438, pp. 191–222.
Miller, C., Thöni, M., Frank, W., Schuster, R., Melcher, F., Meisel, T., Zanetti, A., 2003. Geochemistry and tectonomagmatic affinity of the Yungbwa ophiolite, SW Tibet. Lithos 66, 155–172.

Nicolas, A., Girardeau, J., Marcoux, J., Dupré, B., Wang, X., Zheng, H., Cao, Y., Xiao, X., 1981. The Xigaze ophiolite: a peculiar oceanic lithosphere. Nature 294, 414–417.
Nielsen, R.L., Crum, J., Bourgeois, R., Hascall, K., Forsythe, L.M., Fisk, M.R., Christie, D.M., 1995. Melt inclusions in high-An plagioclase from the Gorda Ridge, an example of local diversity of MORB parent magmas. Contributions to Mineralogy and Petrology 122, 34–50.
Panjasawatwong, Y., Danyushevsky, L.V., Crawford, A.J., Harris, K.L., 1995. An experimental study of effects of melt composition on plagioclase–melt equilibria at 5 and 10 kbar: implications for the origin of magmatic high-An plagioclase. Contributions to Mineralogy and Petrology 118, 420–432.
Pearce, J.A., Deng, W.M., 1988. The ophiolites of the Tibetan geotraverses, Lhasa to Golmud (1985) and Lhasa to Kathamndu (1986). Philosophy Transaction of Royal Society of London A327, 215–238.
Pearce, J.A., Barker, P.F., Edwards, S.J., Parkinson, I.J., Leat, P.T., 2000. Geochemistry and tectonic significance of peridotites from the South Sandwich arc-basin system, South Atlantic. Contributions to Mineralogy and Petrology 139, 36–53.
Piccardo, G.B., 2003. Mantle processes during ocean formation: petrologic records in peridotites from Alpine–Apennine ophiolite. Episode 26, 193–199.
Piccardo, G.B., Zanetti, A., Müntener, O., 2007. Melt/peridotite interaction in the Southern Lanzo peridotite: field, textural and geochemical evidence. Lithos 94, 181–209.
Rampone, E., Piccardo, G.B., Vannucci, R., Bottazzi, P., Ottolini, L., 1993. Subsolidus reactions monitored by trace-element partitioning—the spinel-facies to plagioclase-facies transition in mantle peridotites. Contributions to Mineralogy and Petrology 115, 1–17.
Rampone, E., Piccardo, G.B., Vannucci, R., Bottazzi, P., 1997. Chemistry and origin of trapped melts in ophiolitic peridotites. Geochimica et Cosmochimica Acta 61, 4557–4569.
Rampone, E., Piccardo, G.B., Hofmann, A.W., 2008. Multi-stage melt–rock interaction in the Mt. Maggiore (Corsica, France) ophiolitic peridotites: microstructural and geochemical evidence. Contributions to Mineralogy and Petrology 156, 453–475.
Seyler, M., Bonatti, E., 1997. Regional-scale melt–rock interaction in lherzolitic mantle in the Romanche Fracture Zone (Atlantic Ocean). Earth and Planetary Science Letters 146, 273–287.
Seyler, M., Toplis, M.J., Lorand, J.P., Luguet, A., Cannat, M., 2001. Clinopyroxene microtextures reveal incompletely extracted melts in abyssal peridotites. Geology 29, 155–158.
Sinton, C.W., Christie, D.M., Coombs, V.L., Nielsen, R.L., Fisk, M.R., 1993. Near primary melt inclusions in anorthite phenocrysts from the Galapagos Platform. Earth and Planetary Science Letters 119, 527–537.
Sisson, T.W., Grove, T.L., 1993. Experimental investigations of the role of H_2O in calc–alkaline differentiation and subduction zone magmatism. Contributions to Mineralogy and Petrology 113, 143–166.
Sobolev, A.V., Hofmann, A.W., Kuzmin, D.V., Yaxley, G.M., Arndt, N.T., Chung, S.L., Danyushevsky, L.V., Elliott, T., Frey, F.A., Garcia, M.O., Gurenko, A.A., Kamenetsky, V.S., Kerr, A.C., Krivolutskaya, N.A., Matvienkov, V.V., Nikogosian, I.K., Rocholl, A., Sigurdsson, I.A., Sushchevskaya, N.M., Teklay, M., 2007. The amount of recycled crust in sources of mantle-derived melts. Science 316, 412–417.
Takazawa, E., Frey, F.A., Shimizu, N., Obata, M., 2000. Whoe rock compositional variations in an upper mantle peridotite (Horoman, Hokkaido, Japan): are they consistent with a partial melting process? Geochimica et Cosmochimica Acta 64, 695–716.
Tartarotti, P., Susini, S., Nimis, P., Ottolini, L., 2002. Melt migration in the upper mantle along the Romanche Fracture Zone (Equatorial Atlantic). Lithos 63, 125–149.
van Achterbergh, E., Ryan, C., Jackson, S., Griffin, W.L., 2001. Appendix 3 Data Reduction Software for LA-ICP-MS. In: Sylvester, P. (Ed.), Laser-Ablation-ICPMS in the Earth Sciences: Mineralogical Association of Canada, Short Course, vol. 29, pp. 239–243.
Vannucci, R., Piccardo, G.B., Rivalenti, G., Zanetti, A., Rampone, E., Ottolini, L., Oberti, R., Mazzucchelli, M., Bottazzi, P., 1995. Origin of LREE-depleted amphiboles in the subcontinental mantle. Geochimica et Cosmochimica Acta 59, 1763–1771.
Wang, C.S., Liu, Z.F., Hébert, R., 2000. The Yarlung Zangbo paleo-ophiolite, southern Tibet: implication for dynamic evolution of the Yarlung Zangbo suture zone. Journal of Asian Earth Sciences 18, 651–661.
Xia, B., Yu, H.X., Chen, G.W., Qi, L., Zhao, T.P., Zhou, M.F., 2003. Geochemistry and tectonic environment of the Dagzhuka ophiolite in the Yarlung–Zangbo suture zone, Tibet. Geochemical Journal 37, 311–324.
Xu, D.M., Huang, G.C., Huang, L.Q., Lei, Y.J., Li, L.J., 2006. The origin of mantle peridotites in the Daba–Xiugugabu ophiolite belt, SW Tibet. Geology and Mineral Resource of South China 3, 11–18 (in Chinese with English abstract).
Yin, A., Harrison, T.M., 2000. Geologic evolution of the Himalayan–Tibetan orogen. Annual Review of Earth and Planetary Sciences 28, 211–280.
Zhou, M.F., Robinson, P.T., Malpas, J., Li, Z.J., 1996. Podiform chromitites in the Luobusa ophiolite (southern Tibet): implications for melt–rock interaction and chromite segregation in the upper mantle. Journal of Petrology 37, 3–21.
Zhou, M.F., Robinson, P.T., Malpas, J., Edwards, S.J., Qi, L., 2005. REE and PGE geochemical constraints on the formation of dunites in the Luobusa ophiolite, southern Tibet. Journal of Petrology 46, 615–639.